Distortions in the photocycle of bacteriorhodopsin at moderate dehydration

György Váró and Janos K. Lanyi
Department of Physiology and Biophysics, University of California, Irvine, California 92717 USA

ABSTRACT The photoreaction of bacteriorhodopsin was studied in moderately dehydrated films (relative humidities between 100 and 65%). Time-resolved difference spectra from a gated optical multichannel analyzer, between 100 ns and 100 ms after photoexcitation, were decomposed into sums of difference spectra of the intermediates K, L, M, N, and O, and the kinetics obtained were fitted to various alternative schemes. The data confirm the model of a single reaction sequence with reversible reactions we proposed recently for purple membrane suspensions (Váró, G., and J. K. Lanyi. *Biochemistry.* 1990. 29:2241–2250) but including reversibility also for the reaction K ↔ L in addition to L ↔ M, M ↔ N, and N ↔ O. With increasing dehydration the kinetics were increasingly dominated by the reverse reactions. As before, fitting the data required the existence of two M species in series: L ↔ M_1 → M_2 ↔ N. The M_1 → M_2 reaction was greatly slowed at lower humidities. This step might be the switch for the unidirectional transfer of protons. With increasing dehydration recovery of BR occurred less and less via the N intermediate and increasingly via direct shunts from the two M species. As indicated earlier by electrical measurements with similarly dried bacteriorhodopsin films (Váró, G., and L. Keszthelyi.1983. *Biophys. J.* 43:47–51.) The latter are pathways not necessarily associated with net proton translocation.

INTRODUCTION

Absorption of a photon by light-adapted bacteriorhodopsin (BR[1]) causes the all-*trans* to 13-*cis* isomerization of the retinal chromophore and initiation of a sequence of thermal interconversions of the intermediates designated as J, K, KL[2], L, M, N, and O, leading back to the all-*trans* pigment ("photocycle"). These reactions result in the release of a proton from the exterior surface of BR and the uptake of another on the cytoplasmic side (Lozier et al., 1976), thus, BR functions in the cytoplasmic membrane of *Halobacterium halobium* as a proton pump (for reviews see Stoeckenius et al., 1979; Lanyi, 1984; Khorana, 1988; Oesterhelt and Tittor, 1989). BR is the smallest known protein with an active ion transport role, and the mechanism of proton transport in this system is now beginning to be understood. Clues to the mechanism are found in those steps of the photocycle which are associated with proton transfer (for recent reports, see Braiman et al., 1988; Butt et al., 1989*b*; Tittor et al., 1989; Gerwert et al., 1989; Holz et al., 1989; Otto et al., 1989, 1990): L → M (Schiff base deprotonation and proton release into the medium, mediated by asp-85), M → N (intramolecular proton transfer from asp-96 to the Schiff base), and N → (O) → BR (reprotonation of asp-96 from the medium and reisomerization of the retinal). Additional protonation and deprotonation reactions of M, N, and O have been observed, perhaps related to the protonation of asp-212 (Braiman et al., 1988; Gerwert et al., 1989, 1990), but their pH dependency suggested (Váró and Lanyi, 1990*b*) that they are not essential steps of the vectorial proton translocation process.

It has been known for some time that one of the factors which influences the kinetics of these events in the photocycle is the amount of water associated with BR. The O intermediate was not observable in BR films at humidities <90% (Váró and Keszthelyi, 1983). As humidity was further decreased both the M rise and the M decay deviated increasingly from single exponentials; the former was accelerated whereas the latter was slowed down (Váró and Keszthelyi, 1983; Korenstein and Hess, 1977*b*). The photoelectric signals attributed to these spectroscopic transitions indicated that with decreasing humidity less and less net transfer of protons occurred across the protein (Váró and Keszthelyi, 1983; Kovács and Váró, 1988). Instead, the M → BR pathway seemed to consist of the intramolecular return of the charge (proton) to the Schiff base without the additional movement necessary to breach the full length of the dielectric barrier. These effects were beginning to dominate at ~60% humidity. At still lower water activities

Address correspondence to Dr. Janos K. Lanyi.
Dr. György Váró's permanent address is Biological Research Center of the Hungarian Academy of Sciences, Szeged, Hungary.

[1]*Abbreviation used in this paper:* BR, bacteriorhodopsin.

[2]The late K, or KL, intermediate was described by Shichida et al. (1983). Because our time-resolution does not resolve the early K species we refer to the late species as K rather than KL.

0006-3495/91/02/313/10 $2.00

other phenomena, such as changes in the thermal *cis-trans* isomerization equilibrium (Korenstein and Hess, 1977*a*), spectral shifts (Lazarev and Terpugov, 1980), and the disappearance of the M intermediate (Hildebrandt and Stockburger, 1984; Kovács and Váró, 1988), were also reported.

These findings raised the question that in addition to water at the surface (Zaccai and Gilmore, 1979; Rogan and Zaccai, 1981; Zaccai, 1987; Váró and Eisenstein, 1987; Jaffe and Glaeser, 1987), water molecules might be bound in BR also where they will (*a*) shield charges by solvation, and/or (*b*) participate in proton transfer reactions. Thus, acceleration of the early events in the photocycle at humidities <60% might reflect decreased shielding of separated charges which would make the transient states less stable. The inhibition of the later steps, on the other hand, might reflect decreased hydration of residues critical to proton transfer, such as asp-96 which normally serves to reprotonate the Schiff base.

Some recent reports explain the complex kinetic features of the photocycle in fully hydrated BR by introducing reverse reactions. Thus, the biphasic rise of the M intermediate at high pH was attributed to a reversible L ↔ M reaction (Váró and Lanyi, 1990*a*; Ames and Mathies, 1990). Similarly, the biphasic decay of the M intermediate was attributed to the scheme, M ↔ N → O (Otto et al., 1989; Váró and Lanyi, 1990*a*; Ames and Mathies, 1990; Gerwert et al., 1990). Evidence for N ↔ O equilibration was given earlier by Chernavskii et al. (1989) and Váró et al. (1990). Introducing reversibility into the L → M reaction made it necessary for us to include two sequential M intermediates in the model (Váró and Lanyi, 1990*a*), a feature suggested also by time-resolved FTIR analysis of the photocycle kinetics (Gerwert et al., 1990). We accounted for the opposite pH dependencies of the transient accumulations of the N and O intermediates with a model (Váró et al., 1990) in which the branched O ↔ N → BR pathway dominated at lower pH and the linear N ↔ O → BR pathway dominated at higher pH. We felt that in view of the suggested new models the effects of hydration on the BR photocycle had to be reexamined. Our rationales were the following: (*a*) the earlier data had indicated that gradually removing water from the protein will have specific consequences on the rates of individual transitions. Refining what these changes are would allow critical testing of the proposed photocycle models. Thus, we expected to use the degree of hydration as a variable parameter similarly to how pH (Váró et al., 1990; Váró and Lanyi, 1990*a*) and temperature (Chernavskii et al., 1989; Butt et al., 1989*a*) were used to test models for the BR photocycle. (*b*) Identifying more closely the transitions at which the progressive dehydration has effects would provide new information on the possible role of water in the structure and the photochemical reactions of BR. (*c*) Much of the work on the vibrational spectroscopy of BR intermediates and electrical measurements of charge transfer is with partly dried films of often undefined water content. Description of the photocycle kinetics and its dependency on moisture would provide a useful correlate for these studies.

MATERIALS AND METHODS

Purple membranes were isolated from *Halobacterium halobium* S9 as described before (Oesterhelt and Stoeckenius, 1974). Films were produced by allowing suspensions of these in distilled water to dry on the inside diagonal face of a triangular cuvette. Overnight equilibration with a strip of filter paper, soaked in different salt solutions (Pethig, 1979) and placed into the closed cuvette, was used to regulate the hydration of the BR films. All measurements were at 22°C. The optical density of the films at 570 nm was ~0.7. The films were light-adapted before the measurements.

Time-resolved difference spectra were obtained with a gated optical multichannel analyzer after subnanosecond laser photoexcitation at 580 nm as described before (Zimányi et al., 1989). The film was at a 45° angle to the measuring beam and the laser at 90°. As before, magic angle polarization was used to avoid effects from chromophore reorientation. The laser repetition rate was 0.1–2 Hz depending on the longest relaxation time in the samples, so as to allow sufficient time for the recovery of BR before each photoexcitation. Averaging was over 50–2,000 traces. Data acquisition and reduction were as before (Zimányi et al., 1989; Váró et al., 1990; Váró and Lanyi, 1990*a*), except that, as explained under Results, the measured difference spectra at appropriate times were first used to calculate the best estimates for absolute spectra of the intermediates. Then, a difference spectrum was calculated for each intermediate by subtracting the BR spectrum and the measured time-resolved difference spectra were decomposed into weighted sums of these. The weighting factors gave the time-dependent concentrations of the intermediates. From the same data spectra of the BR without flash excitation were also obtained; these showed that the BR films did not change optically during the flash regime.

As before (Váró et al., 1990; Váró and Lanyi, 1990*a*), kinetic models were fitted by numerical integration of rate equations and systematic iterative search for the rate constants which gave the best fit. The integrations were difficult to do over the required time-range of six orders of magnitude because of the well-known instability of "stiff" differential equations. Conventional approaches such as the Runge-Kutta method (Press et al., 1986) did not give improvement. We overcame the problem by judiciously changing the step sizes in different time-ranges and by replacing formulas with zeros once the concentration of an intermediate became very small.

RESULTS

Calculation of the spectra of the photocycle intermediates and their time-dependent concentrations after flash excitation

Figs. 1 and 2 show measured difference spectra for BR films at 100, 94, 85, and 75% humidities, beginning with

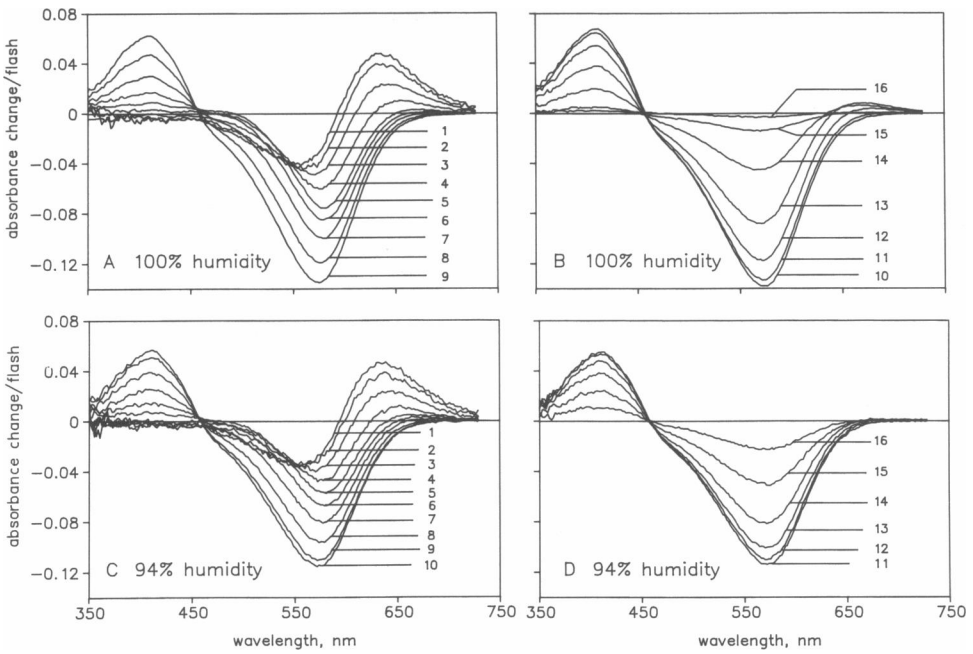

FIGURE 1 Measured difference spectra in BR films at 100% (*A* and *B*) and 94% (*C* and *D*) humidities, at increasing delay times after flash photoexcitation. The measurement was as described in Methods. The numbers 1–17 denote the delay times between the flash and the measurement: 100 ns, 250 ns, 600 ns, 1.5 μs, 4 μs, 10μs, 25μs, 60 μs, 150 μs, 400 μs, 1 ms, 2.5 ms, 6 ms, 15 ms, 40 ms, 100 ms, and 250 ms, in sequence. These traces represent every other spectra measured.

a delay time of 100 ns after the flash. The traces clearly indicate that a large number of interconversions occur before recovery of the BR, and dehydration causes distinct differences. The signal/noise ratio was improved in comparison with previous data of this kind (Váró et al., 1990; Váró and Lanyi, 1990*a*), because the better optical quality of the BR films allowed higher photoconversion at the same laser output energy (estimated at 25%, with 0.13 mJ/flash).

Absolute spectra for K, L, M, N, and O were calculated according to the following strategy. Difference spectra were chosen from the set measured at 100% humidity, at delay times where each of these intermediates was estimated to be represented in maximal amounts. The first three of these were from early delay times where no recovery of BR had yet taken place. Equations were written on the basis that the difference spectra contained absolute spectra for K, L, and M with a positive sign and that of the depleted BR with a negative sign, each multiplied by its transient concentration (x, y, z, w). For every set of the four adjustable parameters x, y, z, w the three measured difference spectra thus yielded three absolute spectra, for K, L, and M. The parameters were then manipulated until the three derived absolute spectra satisfied, simultaneously, the criteria usually used in such fittings (Lozier, 1982): nonnegative absorption, smooth spectra, and shapes which resemble the predicted skewed spectra for rhodopsin-type pigments. The requirement that each displayed spectrum simultaneously satisfy these criteria proved to be surprisingly stringent, i.e., it severly restricted the choice of the variable parameters (to within 1 or 2% of their optimal values). The spectra obtained in this way for K, L, and M (shown in Fig. 3*A*) are remarkably consistent with what is known already about the spectra of these BR intermediates. Spectra for L and M are available from low temperature measurements (Becher et al., 1978) where they could be obtained with fewer assumptions. The reported maximum for L is at 547 nm, whereas its extinction is 50,000 $M^{-1} \cdot cm^{-1}$; for M these values are 412 nm and 44,000 $M^{-1} \cdot cm^{-1}$. Our spectrum for L in Fig. 3*A* has a maximum at 543 nm and an extinction of 48,000 $M^{-1} \cdot cm^{-1}$; for M our values are 408 nm and 45,000 $M^{-1} \cdot cm^{-1}$. It should be noted that the M spectrum contains an unavoidable shoulder near 500 nm which we attribute to a small amount of an additional species of unknown spectrum. This species should have roughly the same kinetics as M. Its presence will introduce an error into the subsequent analysis and the derived model will be incomplete, but we estimate that the error introduced is small. Once the spectra for L and M were accepted the data defined K unambigu-

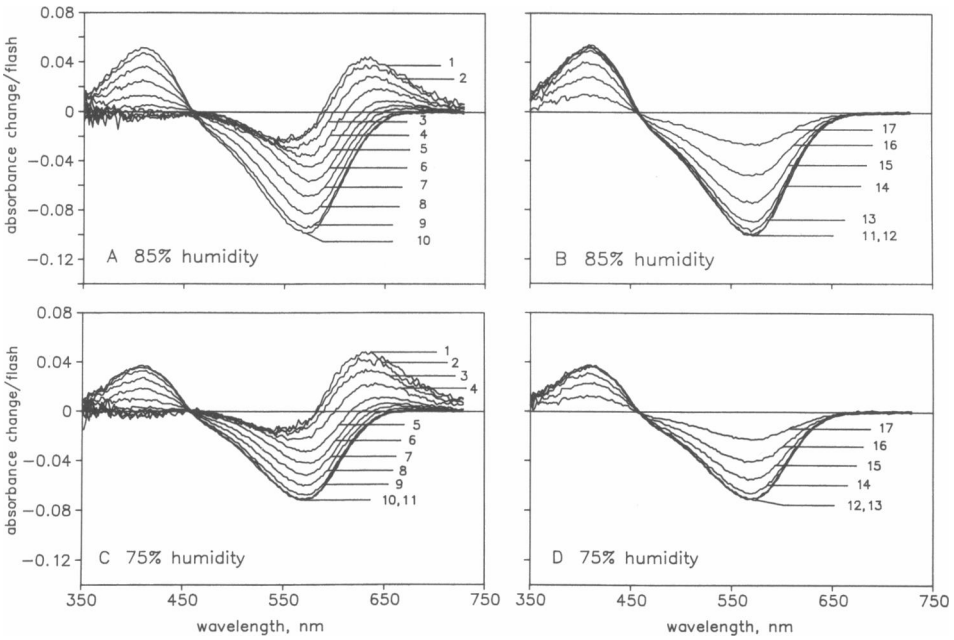

FIGURE 2 Measured difference spectra in BR films at 85% (*A* and *B*) and 75% (*C* and *D*) humidities, at increasing delay times after flash photoexcitation. The measurement was as described in Methods. The numbers 1–17 denote the delay times between the flash and the measurement: 100 ns, 250 ns, 600 ns, 1.5 μs, 4 μs, 10 μs, 25 μs, 60 μs, 150 μs, 400 μs, 1 ms, 2.5 ms, 6 ms, 15 ms, 40 ms, 100 ms, and 250 ms, in sequence. These traces represent every other spectra measured.

ously: its absorption maximum was at 591 nm (Fig. 3 *A*). The ethylenic stretch frequency which correlates with the absorption maximum in the visible is 1,519 cm^{-1} for K, and predicts a maximum at 600 nm (Stern and Mathies, 1985).

After acceptable spectra were obtained for K, L, and M in this way, the process was repeated for two late difference spectra which contained M, N, and O. In these calculations the just obtained M spectrum was used, and the partial recovery of BR was allowed. Earlier reported spectra for N and O had maxima at 550–560 nm and at 615–640 nm, respectively, but because they contained assumptions (Lozier et al., 1975; Kouyama et al., 1988; Zimányi et al., 1989; Hofrichter et al., 1989; Váró et al., 1990) we had to rely on the reported ethylenic stretch frequencies (1,530 cm^{-1} for N in Fodor et al., 1988, and 1,509 cm^{-1} for O in Smith et al., 1983). These frequencies suggested absorption maxima at 556 nm for N and 640 nm for O. We found that only one set of parameters came close to satisfying the criteria listed above and these maxima: our spectra for N and O in Fig. 3 *A* have maxima at 553 and 635 nm, respectively. Subtracting the spectrum of BR from the spectra in Fig. 3 *A* gave individual difference spectra (Fig. 3 *B*), which were then used in fitting the difference spectra measured at all of the humidities tested. This is justified on the grounds that dehydration-dependent spectral shifts are not seen in BR unless the humidity is well below 65% (Lazarev and Terpugov, 1980; measured BR spectra in this study).

The measured difference spectra were assumed to be weighted sums of the individual difference spectra, the weighting factors being the fractional concentrations of the intermediates. The decomposition of each measured spectrum into the component spectra was carried out iteratively until the residual was within the noise level. This could be done for virtually all measured spectra at all humidities. Fig. 4 shows an example of such a fit and the residual on a magnified scale. Because the difference spectra of K, L, and M (and O in other spectra) contributed at different wavelengths to the measured spectrum the decomposition into component spectra was unequivocal. Because of the good signal/noise ratio the decompositions were acceptable even at delay times where L and N coexisted, although with somewhat less confidence because the spectra of these species are similar (Fig. 3).

Fig. 5 *A–D* (points) contain the calculated concentrations of K, L, M, N, O, and BR displayed on a logarithmic time-scale. "BR" in these graphs represents the estimated amount of BR which had entered the photocycle *minus* the sum of the concentrations of

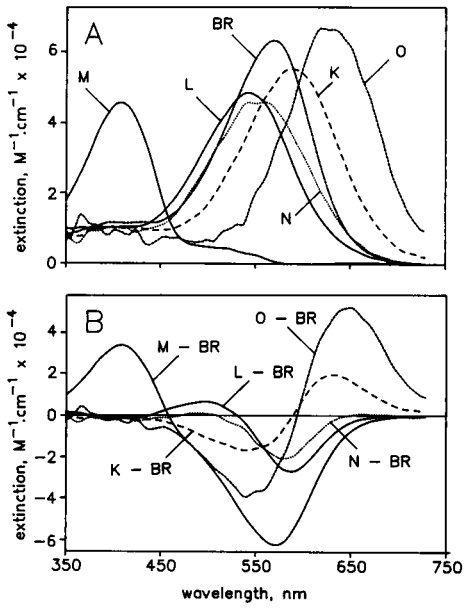

FIGURE 3 Calculated absolute spectra (*A*) and difference spectra (*B*) for the intermediates K, L, M, N, and O. The spectra were calculated, with the assumptions and criteria described in Results, from measured difference spectra at 100% humidity, such as shown in Fig. 1 *A* and *B*. Spectra: (—·—·—) BR, (— — —) K, (———) L, (——) M, (· · ·) N, (— — —) O. The difference spectra represent the absolute spectrum of the intermediate minus the absolute spectrum of BR.

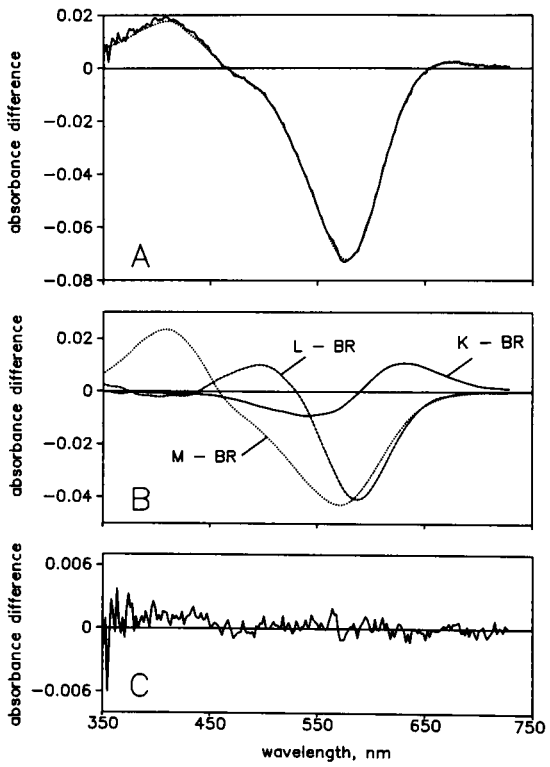

FIGURE 4 An example for the decomposition of a measured difference spectrum into component difference spectra. (*A*) Measured spectrum of BR film at 94% humidity, at 15 μs after photoexcitation, (———); (· · ·), sum of component spectra. (*B*) Component spectra (from Fig. 3 *B*), shown with amplitudes determined by fitting their sum to the measured spectrum in *A*. Spectra: (———), minus BR; (– – –), L minus BR; (· · ·), M minus BR. (*C*) Residual (measured spectrum minus the sum of the spectra in *B*), shown on an enlarged scale.

photointermediates. The latter were results of individual fittings without regard to whether or not they conform to a model. A lack of random fluctuations, and points which lie on smooth, nonnegative curves for the recovery of BR, suggested therefore that the difference spectra in Fig. 3 *B*, obtained from the data at 100% humidity, were applicable at the other humidities and the method in general was at least approximately valid. Qualitatively and independently of a photocycle model the results in Fig. 5 *A–D* show the following: (*a*) with decreasing humidity the nonexponential time-course of the K decay became more and more pronounced. (*b*) The amplitudes of L, M, N, and O did not reach that of the photocycling fraction of BR in any of the data sets. Thus, at all times these species coexisted with other intermediates. (*c*) The rise and decay of M became increasingly separated in time, a result primarily of the slowing of the M decay. The amplitude of M, but even more of L, decreased with decreasing humidity, as reported earlier for dehydrated samples (Lazarev and Terpugov, 1980; Hildebrandt and Stockburger, 1984; Kovács and Váró, 1988). (*d*) With decreasing humidity the transient concentrations of N and O approached zero although their rise and decay relaxation times were not greatly altered. (*e*) With decreasing humidity the recovery of BR became increasingly biphasic.

Fitting of kinetic models to the data, and calculations of individual rate constants

As before (Váró et al., 1990; Váró and Lanyi, 1990*a*), the time-dependent concentrations of the detected intermediates were fitted with numerical solutions of differential equations for various kinetic schemes. We began with the model proposed earlier for purple membrane in suspension at various pH (Váró and Lanyi, 1990*a*), but considered many obvious alternatives as well. Introduction or rejection of a reaction pathway was on grounds dictated by exhaustive search of the rate constants which affected that part of the photocycle. The simplest model which accounted for the data in Fig. 5 is shown in Fig. 6.

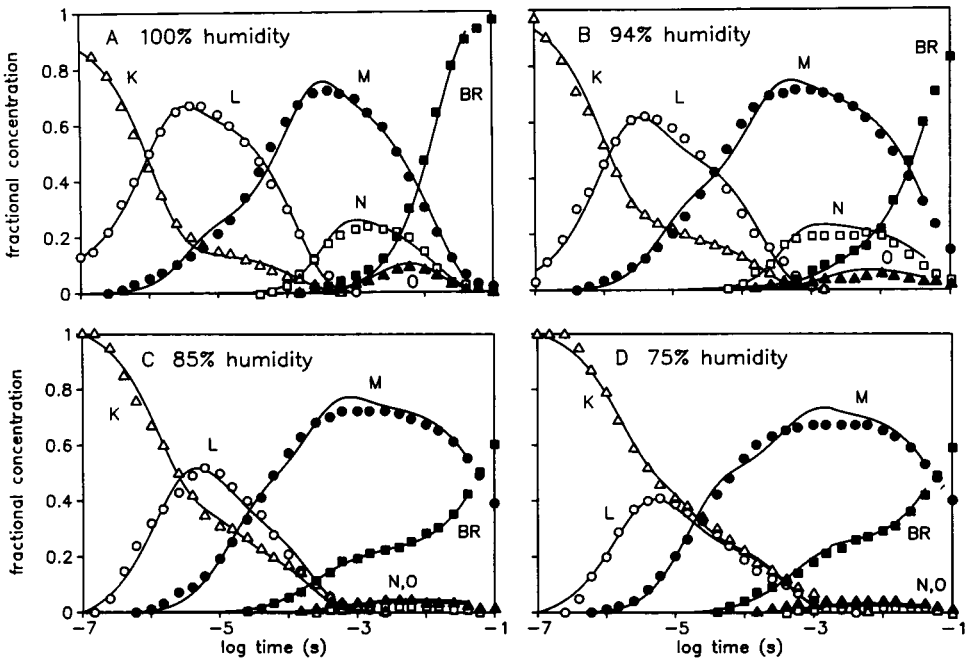

FIGURE 5 Calculated time-dependent concentrations of K, L, M, N, O, and BR, and the best fit of a kinetic model. The BR films were equilibrated with 100% (*A*), 94% (*B*), 85% (*C*), and 75% (*D*) humidity. Symbols: (△) K, (○) L, (●) M (sum of M_1 and M_2), (□) N, (▲) O, (■) BR. The latter represents the sum of detected imtermediates at the indicated times minus the amount of BR that had entered the photocycle. The kinetic model is described in the text and in Fig. 6.

The scheme in Fig. 6 includes several novel, possibly controversial, features, which were justified as follows. (*a*) A single photocycle with multiple reversible reactions, rather than two parallel photocycles. Even more than in our previous report (Váró and Lanyi, 1990*a*), the way in which the kinetics of each intermediate deviated from a single exponential differed from one another. Thus, for example, the amplitudes of the two phases of K decay and the amplitudes of the two phases of BR recovery did not match at all, particularly when data at different humidities were considered. These differences were easily accounted for with reversible interconversions in a single sequence, as in Fig. 6, but not with a model containing two independent photocycles. Earlier we suggested a possible solution by introducing a reverse reaction into one of two simultaneous photocycle sequences (Váró and Lanyi, 1990*a*) but the present data would require additional reverse reactions leading to an unreasonably complex model containing more than two reverse reactions in each of two photocycles. With so many reverse reactions a single cycle suffices. (*b*) Two M species in series, connected by an irreversible reaction. As in the earlier study at high pH (Váró and Lanyi, 1990*a*), we found that K and L, intermediates which are connected to M by the reversible reactions K ↔ L ↔ M, reached near zero concentrations at delay times where M was still highly populated. This is particularly evident at humidities <90% (Fig. 5, *C* and *D*). No set of rate constants was found, given the assumption of a reversible L ↔ M reaction, which allowed this kind of kinetics with only one M: a single M led instead to constant ratios

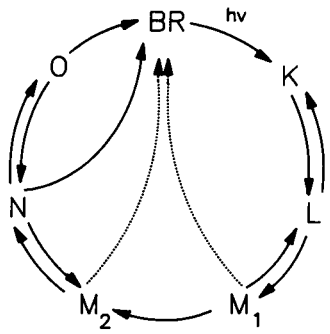

FIGURE 6 Kinetic model used to fit the data in Fig. 5. The model is based on earlier suggested schemes (Váró et al., 1990; Váró and Lanyi, 1990*a*), and its justification is given in the text. All reactions not labeled *hv* are thermal interconversions with measurable rates. The basis for the direct N → BR reaction was given in Váró et al. (1990); although the data at 100% humidity support it, the present work contains little other relevant information for or against this pathway. Kinetics which suggest the existence of M to BR shunts (· · · · · · · · · >) appear only at lower humidities.

for the concentrations of K, L, and M during the entire second half of the photocycle. We distinguish, therefore, between M_1 which is in equilibrium with K and L, and M_2 which is in equilibrium with N and O. What we show in Fig. 5 as M is the sum of M_1 and M_2. This kinetic separation of the first and second halves of the photocycle required that the $M_1 \rightarrow M_2$ reaction not be significantly reversible. (*c*) Direct M → BR reactions at lower humidities. As the humidity was decreased, the recovery of BR began at increasingly earlier times, even though the time-range in which N and O arose and decayed did not change greatly. Thus, at lower humidities the BR recovery became increasingly independent of N and O, and no set of rate constants for these species could model the observed regeneration of BR. Because in these traces the recovery of BR began well before N and O accumulated (cf. Fig. 5, *C* and *D*) we were led to the idea that BR must have been regenerated by shunt pathways directly from M. The strongly biphasic BR recovery required that there be direct pathways from both M species. Remarkably, even though we obtained the rate constant for the $M_1 \rightarrow M_2$ reaction mainly from the relationship of the decays of K and L to M, and this defined the transient accumulations of M_1 and M_2, it was possible to find rate constants for the two M → BR reactions which reproduced the observed BR recovery. The data which suggested two M → BR shunts thus gave further support to the idea of two sequential M states.

The rate constants of the best fit to the model in Fig. 6 (which produced the lines in Fig. 5), are given in Fig. 7 as functions of humidity. From Fig. 7 the following are evident: (*a*) rate constants which described reactions leading away from L ($k_{L/K}$ and $k_{L/M1}$) were relatively little affected by humidity but those for reactions which produced L ($k_{K/L}$ and $k_{M1/L}$) decreased with decreasing water content. This was the reason that the accumulation of L progressively decreased with dehydration (Fig. 5 *A–D*). (*b*) The rate constant of the conversion of M_1 to M_2 ($k_{M1/M2}$) decreased very considerably with decreasing water content, particularly at lower humidities. This produced the appearance of biphasic recovery for BR <90% humidity. (*c*) The rate constants of the recovery of BR directly from the two M species ($k_{M1/BR}$ and $k_{M2/BR}$) were unmeasurably small at 100% humidity, increased as the water content decreased, but became smaller again as the humidity was lowered <80%. These processes seemed to be governed, therefore, by two different moisture-dependent effects. (*d*) The rate constant for the usual decay route of M via N ($k_{M2/N}$) decreased with decreasing humidity, effectively closing this pathway at 65%. The rate constants of the other reactions which involved N and O (not shown in Fig. 7) were also evaluated but they were not reliable at the lower humidities where N and O were barely observable.

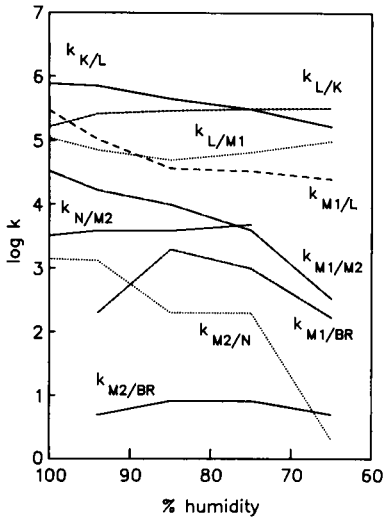

FIGURE 7 Calculated rate constants for the reactions in Fig. 6 at different humidities. The rate constants are from fitting the model to the data in Fig. 5 *A–D*; the data for 65% humidity were not shown. The rate constants refer to the following reactions: $k_{K/L}$, K → L (———); $k_{L/K}$, L → K (- - -); $k_{L/M1}$, L → M_1 (· · ·); $k_{M1/L}$, M_1 → L (— — —); $k_{M1/M2}$, M_1 → M_2 (— · — · —); $k_{M2/N}$, M_2 → N (· · ·); $k_{N/M2}$, N → M_2 (———); $k_{M1/BR}$, M_1 → BR (— · · — · · —); $k_{M2/BR}$, M_2 → BR (———). Although they could not be exactly evaluated, $k_{M1/BR}$ and $k_{M2/BR}$ were very low at 100% humidity; the value of $k_{N/M2}$ at 65% humidity is uncertain. Rate constants for reactions after N are not shown.

The calculations did indicate, however, that both forward and reverse rate constants in the N ↔ O equilibration greatly increased, and the rate constants for the recovery of BR from N and O greatly decreased, with decreasing humidity.

DISCUSSION

The interpretation of time-resolved difference spectra for BR is hindered by lack of assumption-free methodology to (*a*) derive absorption spectra for each observed intermediate of the photocycle, and (*b*) fit the time-dependent concentrations of these to a unique model defined by kinetic differential equations. We dealt with this problem by first calculating best estimates for the absorption spectra of the intermediates (Fig. 3 *A*) from selected time-points in one data-set, using severely restricting criteria (cf. Results). The calculated spectra agreed well with what is known about these spectra from earlier, independent information in the literature. The measured difference spectra in all of the data-sets were then decomposed into sums of the calculated difference spectra; the weighting factors gave the time-dependent concentrations of the intermediates (Fig. 5 *A–D*). Models of the photocycle were then evaluated by comparing

their numerical solutions to the data using systematic search strategies to arrive at the model which explained the data. Because some subjective judgment had to be used in accepting the intermediate spectra (Fig. 3 *A*), their accuracy was the major factor in the accuracy of the subsequent kinetic analysis. The other, minor factors were possible ambiguities in the decomposition into difference spectra (Fig. 4) and the rigor of the parameter search in ruling out alternative kinetic schemes. It was reassuring that the analysis produced consistency with respect to both the sum of the intermediates at various times (cf. Fig. 5) and the smooth way the estimated rate constants varied with the humidity of the samples (Fig. 7).

The photocycle kinetics of a BR film at 100% humidity were similar to the kinetics of purple membranes in aqueous suspension reported earlier (Váró and Lanyi, 1990*a*). The ratio of amplitudes for the N and O intermediates (Fig. 5 *A*) identified the effective pH in this sample as 7–7.5. The kinetics were characterized by extensive temporal overlap of all of the intermediates, and significant deviations from single exponentials, effects which became exaggerated in purple membrane suspensions at higher pH (Váró and Lanyi, 1990*a*). Data for the films were analyzed for K as well, and they suggested reversibility for the K to L reaction. Thus, the model in Fig. 6 includes the K ↔ L, as well as the L ↔ M, M ↔ N, and N ↔ O interconversions proposed earlier. The calculated values for $k_{K/L}$, $k_{L/M}$, $k_{M/L}$, and $k_{M1/M2}$ were quite similar to those determined earlier for purple membrane suspensions at pH 7.5, but $k_{M2/N}$ and $k_{N/M2}$ were about an order of magnitude higher than the earlier values. Thus, interestingly, proton exchange between the Schiff base and asp-96 seems to be much faster in fully hydrated BR films than in aqueous suspensions.

The results suggested that with progressive dehydration the photocycle kinetics undergo important changes. The major distortions were the following: (*a*) Because the $M_1 \rightarrow M_2$ reaction was greatly slowed the accumulation of the early intermediates was dominated by the reverse reactions K ↔ L ↔ M_1. (*b*) Because the $M_2 \rightarrow N$ reaction was drastically slowed and direct $M_1 \rightarrow$ BR and $M_2 \rightarrow$ BR reactions began to appear the recovery of BR was increasingly through these shunts rather than through the usual M → N → (O) → BR pathway. The proposed shunt pathways will not necessarily result in proton translocation, because electrical measurements of semi-dry BR films had indicated that the net charge transfer decreased with decreasing water content (Váró and Keszthelyi, 1983). This would happen if in the shunt reaction the proton is returned to the Schiff base from the same residue which had received it during the deprotonation. Because the spectrum of BR did not change during the measurements where each of many flash illuminations cycled as much as 25% of the sample, we assume that the shunt pathways produced all-*trans* rather than 13-*cis* BR.

We feel that the present results strongly argue in favor of the model in Fig. 6 for dehydrated BR films. The results also confirm the main features of the general model we proposed for BR under other conditions (Váró and Lanyi, 1990*a*): the existence of reversible reactions in a single photocycle, and two sequential M intermediates connected by an irreversible reaction. Two parallel M species have been proposed before to explain the nonexponential rise and decay of M (e.g., Kouyama et al., 1988; Butt et al., 1989*a*). It should be emphasized that the rationale for the proposed two sequential M species is different and found mainly in the kinetics of the decay of L, as described above.

It is a novel finding that with drying the ratio of forward to reverse photocycle reactions changed significantly. The results mean that the differences in free energy levels which separate several of the intermediates change with dehydration. The free energy levels associated with the retinal bond rotations in BR, (e.g., Orlandi and Schulten, 1979; Tavan et al., 1985), will be influenced by the protein matrix. At high water content this influence will not necessarily appear as a dissipative effect, because the protein is in a relatively mobile environment and can assume a large number of conformational states. Most of the water in purple membranes is on the surface, and associated with lipid headgroups (Zaccai and Gilmore, 1979; Rogan and Zaccai, 1981; Zaccai, 1987; Váró and Eisenstein, 1987; Jaffe and Glaeser, 1987). Importantly, dehydration was seen to cause decrease in in-plane spacing due to condensation of the lipid chains and it was proposed that this will restrict motions of the protein (Zaccai, 1987). Thus, with increasing dehydration the configurational motions of the retinal might be less and less accomodated by appropriate conformational motions of the protein. This qualitative picture provides a ready explanation also for the appearance of the proposed shunt pathways for the reprotonation of the Schiff base, which would be allowed by condensed protein conformations not highly populated at higher degrees of hydration.

The existence of reversible reactions explains the earlier observation that an external electric field changed the integrated current signal associated with the L → M transition, i.e. the apparent amount of M produced in the cycle, while the apparent amount of L was not greatly changed (Groma et al., 1988). We calculated the consequence of an electric field on the photocycle kinetics, using the model in Fig. 6 and the Nernst relationship, $k(E) = k \cdot \exp(-\text{constant} \cdot E)$, where $k(E)$ and k are the rate constants with and without electric

field, respectively, E is the external electric field, and the constant is determined by the distance of charge translocation in each transition (see Váró and Keszthelyi, 1985). The result of this simulation was that the accumulation of M, but not L, was greatly changed by the electric field, as indeed experimentally found (Groma et al., 1988).

The two sequential M states have been proposed on the basis of kinetic evidence in this and an earlier work (Váró and Lanyi, 1990*a*), as well as in another analysis (Gerwert et al., 1990). Two distinguishable M species have been proposed earlier, however, on the basis of small differences found in the absorption maxima near 410 nm (Hess and Kuschmitz, 1977), and from C^{13} NMR spectra which argue for one M with C = N *syn* and another with C = N *anti* configuration (Smith et al., 1989). The latter finding seems consistent with an analysis of time-resolved resonance energy transfer between the retinal and a fluorescent membrane label, from which the existence of two (interpreted as parallel) M species with different retinal orientations was proposed (Hasselbacher and Dewey, 1986). However, resonance Raman spectra showed that M contained a C = N *anti* chromophore during both rapid and slow phases of decay (Ames et al., 1989). *Syn-anti* isomerization during the M state is somewhat unlikely also, in view of the fact that both L and N contain the *anti* configuration (Smith et al., 1984; Fodor et al., 1988). Rotation around the C14–C15 single bond (Gerwert and Siebert, 1986) might account for the $M_1 \rightarrow M_2$ transition. Alternatively, the two M species might differ in protein conformation (Gerwert et al., 1985). Fodor et al. (1988) had proposed that the photocycle contains an essential protein conformational change. The strong inhibition of the $M_1 \rightarrow M_2$ reaction by dehydration (Fig. 7) is consistent with either of these alternatives if significant motion is associated with them. We have suggested (Váró and Lanyi, 1990*a*) that the detected irreversible step at this place in the photocycle separating the reversible L $\leftrightarrow$ M_1 and $M_2 \leftrightarrow$ N reactions plays the role of the switch for directing the unidirectional transfer of protons from the cytoplasmic to the external side of the membrane barrier.

This work was supported by grants from the National Institutes of Health (GM 29498) and the Department of Energy (DE-FGOER 13525).

Received for publication 19 March 1990 and in final form 11 October 1990.

REFERENCES

Ames, J. B., and R. A. Mathies. 1990. The role of back-reactions and proton uptake during the N --> O transition in bacteriorhodopsin's photocycle: a kinetic resonance Raman study. *Biochemistry.* 29:7181–7190.

Ames, J. B., S. P. A. Fodor, R. Gebhard, J. Raap, M. M. van den Berg, J. Lugtenburg, and R. A. Mathies. 1989. Bacteriorhodopsin's M_{412} intermediate contains a 13-*cis*, 14-s-*trans*, 15-*anti*-retinal Schiff base chromophore. *Biochemistry.* 28:3681–3687.

Becher, B., F. Tokunaga, and T. G. Ebrey. 1978. Ultraviolet and visible absorption spectra of the purple membrane protein and the photocycle intermediates. *Biochemistry.* 17:2293–2300.

Braiman, M. S., T. Mogi, T. Marti, L. J. Stern, H. G. Khorana, and K. J. Rothschild. 1988. Vibrational spectroscopy of bacteriorhodopsin mutants: light-driven proton transport involves protonation changes of aspartate residues 85, 96, and 212. *Biochemistry.* 27:8516–8520.

Butt, H.-J., K. Fendler, A. Dér, and E. Bamberg. 1989*a*. Temperature jump study of charge translocation during the bacteriorhodopsin photocycle. *Biophys. J.* 56:851–859.

Butt, H. J., K. Fendler, E. Banberg, J. Tittor, and D. Oesterhelt. 1989*b*. Aspartic acids 96 and 85 play a central role in the function of bacteriorhodopsin as a proton pump. *EMBO (Eur. Mol. Biol. Organ.) J.* 8:1657–1663.

Chernavskii, D. S., I. V. Chizhov, R. H. Lozier, T. M. Murina, A. M. Prokhorov, and B. V. Zubov. 1989. Kinetic model of bacteriorhodopsin photocycle: pathway from M state to bR. *Photochem. Photobiol.* 49:649–653.

Fodor, S. P., J. B. Ames, R. Gebhard, E. M. van der Berg, W. Stoeckenius, J. Lugtenburg, and R. A. Mathies. 1988. Chromophore structure in bacteriorhodopsin's N intermediate: implications for the proton pumping mechanism. *Biochemistry.* 27:7097–7101.

Gerwert, K., and F. Siebert. 1986. Evidence for light-induced 13-*cis*, 14-s-*cis* isomerization in bacteriorhodopsin obtained by FTIR difference spectroscopy using isotopically labeled retinals. *EMBO (Eur. Mol. Biol. Organ.) J.* 5:805–811.

Gerwert, K., R. Rodriquez-Gonzales, and F. Siebert. 1985. Time-resolved infrared spectroscopy applied to photobiological systems. *In* Time-resolved Vibrational Spectroscopy. A. Laubereau and M. Stockburger, editors. Springer-Verlag, Berlin. 263–268.

Gerwert, K., B. Hess, J. Soppa, and D. Oesterhelt. 1989. Role of aspartate-96 in proton translocation by bacteriorhodopsin. *Proc. Natl. Acad. Sci. USA* 86:4843–4947.

Gerwert, K., G. Souvignier, and B. Hess. 1990. Light-induced protonation changes of protein side-groups, chromophore isomerization and backbone motion of bacteriorhodopsin simultaneously monitored by time-resolved FTIR spectroscopy. *Proc. Natl. Acad. Sci. USA.* In press.

Groma, G. I., G. Váró, and L. Keszthelyi. 1988. Effect of the electric field on the photocycle of bacteriorhodopsin. *In* Molecular Physiology of Retinal Proteins. T. Hara, editor. Yamada Science Foundation. Osaka, Japan. 97–102.

Hasselbacher, C. A., and T. G. Dewey. 1986. Changes in retinal position during the bacteriorhodopsin photocycle: a resonance energy-transfer study. *Biochemistry.* 25:6236–6243.

Hess, B., and D. Kuschmitz. 1977. The photochemical reaction of the 412 nm chromophore of bacteriorhodopsin. *FEBS. (Fed. Eur. Biochem. Soc.) Lett.* 74:29–34.

Hildebrandt, P., and M. Stockburger. 1984. Role of water in bacteriorhodopsin's chromophore: resonance Raman study. *Biochemistry.* 23:5539–5548.

Hofrichter, J., E. R. Henry, and R. H. Lozier. 1989. Photocycles of bacteriorhodopsin in light- and dark-adapted purple membrane studied by time-resolved absorption spectroscopy. *Biophys. J.* 56:693–706.

Holz, M., L. A. Drachev, T. Mogi, H. Otto, A. D. Kaulen, M. P. Heyn, V. P. Skulachev, and H. G. Khorana. 1989. Replacement of aspartic acid-96 by asparagine in bacteriorhodopsin slows both the decay of the M intermediate and the associated proton movement. *Proc. Natl. Acad. Sci. USA*. 86:2167–2171.

Jaffe, J. S., and R. M. Glaeser. 1987. Difference Fourier analysis of "surface features" of bacteriorhodopsin using glucose-embedded and frozen-hydrated purple membrane. *Ultramicroscopy*. 23:17–28.

Khorana, H. G. 1988. Bacteriorhodopsin, a membrane protein that uses light to translocate protons. *J. Biol. Chem.* 263:7439–7442.

Korenstein, R., and B. Hess. 1977*a*. Hydration effects on *cis-trans* isomerization of bacteriorhodopsin. *FEBS. (Fed. Eur. Biochem. Soc.) Lett.* 82:7–11.

Korenstein, R., and B. Hess. 1977*b*. Hydration effects on the photocycle of bacteriorhodopsin in thin layers of purple membrane. *Nature (Lond.)*. 270:184–186.

Kouyama, T., A. Nasuda-Kouyama, A. Ikegami, M. K. Mathew, and W. Stoeckenius. 1988. Bacteriorhodopsin photoreaction: identification of a long-lived intermediate N (P, R_{350}) at high pH and its M-like photoproduct. *Biochemistry*. 27:5855–5863.

Kovács, I., and G. Váró. 1988. Charge motion in vacuum-dried bacteriorhodopsin. *J. Photochem. Photobiol. B Biol.* 1:469–474.

Lanyi, J. K. 1984. Bacteriorhodopsin and related light-energy converters. *In* Comparative Biochemistry: Bioenergetics. L. Ernster, editor. 315–350, Elsevier Science Publishers B. V., Amsterdam. 315–350.

Lazarev, Y. A., and E. L. Terpugov. 1980. Effect of water on the structure of bacteriorhodopsin and photochemical processes in purple membranes. *Biochim. Biophys. Acta*. 590:324–338.

Lozier, R. H. 1982. Rapid kinetic optical absorption spectroscopy of bacteriorhodopsin photocycles. *Methods Enzymol.* 88:133–162.

Lozier, R. H., R. A. Bogomolni, and W. Stoeckenius. 1975. Bacteriorhodopsin: a light-driven proton pump in *Halobacterium halobium*. *Biophys. J.* 15:955–963.

Lozier, R. H., W. Niederberger, R. A. Bogomolni, S. Hwang, and W. Stoeckenius. 1976. Kinetics and stoichiometry of light-induced proton release and uptake from purple membrane fragments, *Halobacterium halobium* cell envelopes, and phospholipid vesicles containing oriented purple membrane. *Biochim. Biophys. Acta*. 440:545–556.

Oesterhelt, D., and W. Stoeckenius. 1974. Isolation of the cell membrane of *Halobacterium halobium* and its fractionation into red and purple membrane. *Methods Enzymol.* 31:667–678.

Oesterhelt, D., and J. Tittor. 1989. Two pumps, one principle: light-driven ion transport in halobacteria. *TIBS (Trends Biochem. Sci.)* 14:57–61.

Orlandi, G., and K. Schulten. 1979. Coupling of sterochemistry and proton donor-acceptor properties of a Schiff base. A model of a light-driven proton pump. *Chem. Phys. Lett.* 64:370–374.

Otto, H., T. Marti, M. Holz, T. Mogi, M. Lindau, H. G. Khorana, and M. P. Heyn. 1989. Aspartic acid-96 is the internal proton donor in the reprotonation of the Schiff base of bacteriorhodopsin. *Proc. Natl. Acad. Sci. USA* 86:9228–9232.

Otto, H., T. Marti, M. Holz, T. Mogi, L. J. Stern, F. Engel, H. G. Khorana, and M. P. Heyn. 1990. Substitution of amino acids Asp-85, Asp-212, and Arg-82 in bacteriorhodopsin affects the proton release phase of the pump and the pK of the Schiff base. *Proc. Natl. Acad. Sci. USA*. 87:1018–1022.

Pethig, R. 1979. Dielectric and Electronic Properties of Biological Materials. John Wiley & Sons Inc., New York. 126 pp.

Press, W. H., B. P. Flannery, S. A. Teukolsky, and W. T. Vetterling. 1986. Numerical Recipes. Cambridge University Press, Cambridge. 550–560.

Rogan, P. K., and G. Zaccai. 1981. Hydration in purple membrane as a function of relative humidity. *J. Mol. Biol.* 145:281–284.

Shichida, Y., S. Matuoka, Y. Hidaka, and T. Yoshizawa. 1983. Absorption spectra of intermediates of bacteriorhodopsin measured by laser photolysis at room temperatures. *Biochim. Biophys. Acta*. 723:240–246.

Smith, S. O., J. A. Pardoen, P. P. J. Mulder, B. Curry, J. Lugtenburg, and R. Mathies. 1983. Chromophore structure in bacteriorhodopsin's O_{640} photointermediate. *Biochemistry*. 22:6141–6148.

Smith, S. O., A. B. Myers, J. A. Pardoen, C. Winkel, P. P. J. Mulder, J. Lugtenburg, and R. A. Mathies. 1984. Determination of retinal Schiff base configuration in bacteriorhodopsin. *Proc. Natl. Acad. Sci. USA*. 81:2055–2059.

Smith, S. O., J. Courtin, E. van der Berg, C. Winkel, J. Lugtenburg, J. Herzfeld, and R. G. Griffin. 1989. Solid-state 13C NMR of the retinal chromophore in photointermediates of bacteriorhodopsin: characterization of two forms of M. *Biochemistry*. 28:237–243.

Stern, D., and R. A. Mathies. 1985. Picosecond and nanosecond resonance Raman evidence for structural relaxation in bacteriorhodopsin's primary photoproduct. *In* Time-resolved Vibrational Spectroscopy. A. Lauberaeu and M. Stockburger, editors. Springer-Verlag, Berlin. 250–254.

Stoeckenius, W., R. H. Lozier, and R. A. Bogomolni. 1979. Bacteriorhodopsin and the purple membrane of halobacteria. *Biochim. Biophys. Acta*. 505:215–278.

Tavan, P., K. Schulten, and D. Oesterhelt. 1985. The effect of protonation and electrical interactions on the sterochemistry of retinal Schiff bases. *Biophys. J.* 47:415–430.

Tittor, J., C. Soell, D. Oesterhelt, H.-J. Butt, and E. Bamberg. 1989. A defective proton pump, point-mutated bacteriorhodopsin Asp96 → Asn is fully reactivated by azide. *EMBO (Eur. Mol. Biol. Organ.) J.* 8:3477–3482.

Váró, G., and L. Eisenstein. 1987. Infrared studies of water induced conformational changes in bacteriorhodopsin. *Eur. J. Biochem.* 14:163–168.

Váró, G., and L. Keszthelyi. 1983. Photoelectric signals from dried oriented purple membranes of *Halobacterium halobium*. *Biophys. J.* 43:47–51.

Váró, G., and L. Keszthelyi. 1985. Arrhenius parameters of the bacteriorhodopsin photocycle in dried oriented samples. *Biophys. J.* 47:243–246.

Váró, G., and J. K. Lanyi. 1990*a*. Pathways of the rise and decay of the M photointermediate of bacteriorhodopsin. *Biochemistry*. 29:2241–2250.

Váró, G., and J. K. Lanyi. 1990*b*. Protonation and deprotonation of the M, N, and O intermediates during the bacteriorhodopsin photocycle. *Biochemistry*. 29:6858–6865.

Váró, G., A. Duschl, and J. K. Lanyi. 1990. Interconversions of the M, N, and O intermediates of the bacteriorhodopsin photocycle. *Biochemistry*. 29:3798–3804.

Zaccai, G. 1987. Structure and hydration of purple membranes in different conditions. *J. Mol. Biol.* 194:569–572.

Zaccai, G., and D. J. Gilmore. 1979. Areas of hydration in the purple membrane of *Halobacterium halobium*: a neutron diffraction study. *J. Mol. Biol.* 132:181–191.

Zimányi, L., L. Keszthelyi, and J. K. Lanyi. 1989. Transient spectroscopy of bacterial rhodopsins with optical multichannel analyser. 1. Comparison of the photocycles of bacteriorhodopsin and halorhodopsin. *Biochemistry*. 28:5165–5172.